AGU PUBLICATIONS

Paleoceanography

RESEARCH ARTICLE
10.1002/2016PA002931

Key Points:
- Bamboo coral C and O isotope vital effects can be accounted for when they are referenced to appropriate abiogenic fractionations
- Successfully correcting for vital effects allows coral-based temperatures to be estimated from the abiogenic relationship
- Greater incorporation of metabolic C may complicate the interpretation of Atlantic coral data

Supporting Information:
- Supporting Information S1

Correspondence to:
C. Saenger,
csaenger@uw.edu

Citation:
Saenger, C., and J. M. Watkins (2016), A refined method for calculating paleotemperatures from linear correlations in bamboo coral carbon and oxygen isotopes, *Paleoceanography*, *31*, 789–799, doi:10.1002/2016PA002931.

Received 3 FEB 2016
Accepted 30 MAY 2016
Accepted article online 3 JUN 2016
Published online 24 JUN 2016

A refined method for calculating paleotemperatures from linear correlations in bamboo coral carbon and oxygen isotopes

Casey Saenger[1] **and James M. Watkins**[2]

[1]Joint Institute for the Study of the Atmosphere and Ocean, University of Washington, Seattle, Washington, USA,
[2]Department of Geological Sciences, University of Oregon, Eugene, Oregon, USA

Abstract Bamboo corals represent an emerging paleoclimate archive with the potential to record variability at intermediate depths throughout much of the global ocean. Realizing this potential has been complicated by biologically mediated vital effects, which are evident in linear correlations of skeletal carbon (δ^{13}C) and oxygen (δ^{18}O) isotope composition. Previous efforts to develop a bamboo coral δ^{18}O paleothermometer by accounting for such vital effects have not been completely successful as they still rely on empirical calibrations that are offset from the temperature dependence of abiogenic experiments. Here we describe an approach that better corrects for bamboo coral vital effects and allows paleotemperatures to be calculated directly from the abiogenic temperature dependence. The success of the method lies in calculating apparent equilibrium carbon and oxygen isotope fractionation at the temperature, pH, and growth rate of each coral, as well as in the use of model II regressions. Rigorous propagation of uncertainty suggests typical errors of ±2–3°C, but in select cases errors as low as ±0.65°C can be achieved for densely sampled and strongly correlated data sets. This lower limit approaches the value attributed to uncertainty in pH and growth rate estimates alone, as predicted by a series of pseudoproxy experiments. The incorporation of isotopically light metabolic CO_2 appears to be negligible in most Pacific corals, but may be significant in Atlantic specimens, potentially requiring an additional correction. The success of the method therefore hinges on how well complex environmental systems and biomineralization strategies are constrained, with the most reliable temperatures occurring when calcifying fluid pH, growth rate, and incorporation of metabolic carbon into skeletal calcite are constrained using multiple geochemical proxies.

1. Introduction

The intermediate ocean is an important heat sink that accounts for approximately a third of Earth's warming since the middle twentieth century [*Levitus et al.*, 2012]. Variations in the amount of heat sequestered in the intermediate ocean can have widespread climatic impacts, and have been implicated in the controversial recent slowdown of global warming [*Chen and Tung*, 2014]. Whether these trends are anomalous in the context of long-term natural variability is difficult to determine from the brief observational record alone, making intermediate ocean paleotemperature reconstructions particularly valuable.

Deep sea corals represent promising archives of past subsurface temperature variability due to their global distribution, longevity, and ability to be dated with radiometric techniques [*Robinson et al.*, 2014]. Bamboo corals (*Keratoisis* and *Isidella* sp.) are common at depths of ~100–3500 m [*Etnoyer and Morgan*, 2005; *Farmer et al.*, 2015a; *Hill et al.*, 2011; *Kimball et al.*, 2014] where they precipitate skeletons of calcite internodes and organic nodes throughout multidecadal to century-long lifespans [*Andrews et al.*, 2009; *Farmer et al.*, 2015b; *Sherwood and Edinger*, 2009]. Bamboo coral calcification appears to occur at near ambient pH with little biologically mediated up regulation [*Farmer et al.*, 2015a] (Figure 1), leading to modest linear extension rates of ~12–160 μm/yr [*Andrews et al.*, 2009; *Farmer et al.*, 2015b; *Thresher et al.*, 2009]. Expressed as calcification rates (R), this is equivalent to $\log R \approx -7.3$ mol/m^2/s assuming a calcite density of 2.71 g/cm^3 [*DeFoe and Compton*, 1925] (Figure 1), and is sufficiently fast to potentially yield annual- to decadal-scale paleoenvironmental reconstructions that reach into the preindustrial era. Geochemical variations in bamboo corals have been explored as proxies for marine nutrients [*LaVigne et al.*, 2011], pH [*Farmer et al.*, 2015a], seawater trace metal concentration [*Hill et al.*, 2012], carbon export [*Hill et al.*, 2014], and especially temperature [*Hill et al.*, 2011; *Kimball et al.*, 2014; *Thresher et al.*, 2004, 2010].

The reconstruction of temperature from bamboo corals has been complicated by the impact of variables other than temperature on traditional paleothermometers. Although the magnesium to calcium ratio (Mg/Ca) of bamboo coral calcite internodes is relatively reproducible [*Sinclair et al.*, 2011] and shows a

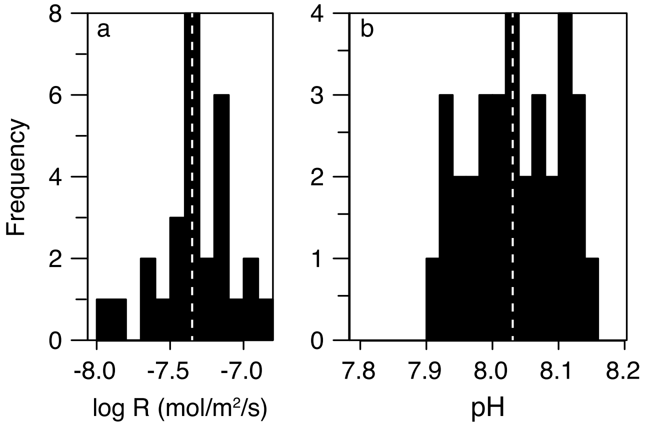

Figure 1. Histogram of literature values for bamboo coral (a) growth rate and (b) pH. Growth rates are based on radiocarbon and ^{210}Pb dating [*Andrews et al.*, 2009; *Farmer et al.*, 2015b; *Hill et al.*, 2011; *Roark et al.*, 2005; *Sherwood and Edinger*, 2009]. The pH values are based on δ^{11}B [*Farmer et al.*, 2015a]. Vertical dashed lines mark median values.

weak positive correlation with temperature [*Thresher et al.*, 2010], this relationship differs from that of abiogenic precipitation experiments [*Mucci*, 1987; *Oomori et al.*, 1987] and comparable coral genera [*Bond et al.*, 2005; *Sherwood et al.*, 2005; *Weinbauer et al.*, 2000]. Similarly, the oxygen isotope composition (δ^{18}O) of bamboo corals exhibits large intercoral and intracoral variations that cannot be explained by temperature and are better explained by biologically mediated and/or kinetic effects [*Hill et al.*, 2011; *Kimball et al.*, 2014].

Nonequilibrium δ^{18}O values in corals are often accompanied by proportional deviations in their carbon isotope composition (δ^{13}C) that produce strong linear correlations between the two variables that may be explained by a common mechanism [e.g., *Adkins et al.*, 2003; *Emiliani et al.*, 1978; *McConnaughey*, 1989]. *Smith et al.* [2000] demonstrated that δ^{18}O-δ^{13}C trends in aragonitic azooxanthellate corals often had similar slopes but exhibited systematically offset intercepts that were correlated with temperature. Using this observation, they suggested that by extrapolating trends to the point where coral δ^{13}C equaled that of the surrounding dissolved inorganic carbon (DIC) (i.e., $\delta^{13}C_{coral}$-$\delta^{13}C_{DIC} = 0‰$), one could calculate the $\delta^{18}O_{coral}$-$\delta^{18}O_{water}$ at apparent equilibrium [*Grossman and Ku*, 1986], which could in turn be used to calculate the mean growth temperature over a coral's lifespan.

Recent work has applied this empirical "lines method" to calcitic bamboo corals in the Family *Isididae*, which also exhibit strong linear trends in δ^{18}O-δ^{13}C [*Hill et al.*, 2011; *Kimball et al.*, 2014]. Extrapolating a model I regression to $\delta^{13}C_{coral}$-$\delta^{13}C_{DIC} = 0‰$, yielded $\delta^{18}O_{coral}$-$\delta^{18}O_{water}$ with a temperature sensitivity similar to the abiogenic calcite relationship of *Kim and O'Neil* [1997], but with a systematically offset intercept [*Kimball et al.*, 2014]. It was suggested that coral growth temperature could be calculated from this empirical relationship, but this approach was partially circular given that the coral for which temperature was being calculated was not independent of the paleotemperature calibration. Furthermore, it was proposed that the 95% confidence intervals of this empirical relationship could be used to calculate the uncertainties in coral-based temperatures of ±0.7°C for corals growing close to 2°C and ±1.4°C for those growing near 11°C [*Kimball et al.*, 2014].

Despite making progress toward circumventing vital effects, previous methods for doing so can be refined. First, a method that successfully accounts for vital effects should not rely solely on an empirical calibration but rather should use independent abiogenic calcite experiments as a reference frame. Second, both δ^{18}O and δ^{13}C possess analytical errors that are not accounted for in the model I regressions typically used to establish δ^{18}O-δ^{13}C trends (Figure 2a), making model II regression techniques preferable. Although, *Hill et al.* [2011] correctly pointed out that the difference between model I and II regressions are negligible for strong correlations, model I techniques produce an erroneously shallow slope for weaker correlations that can lead to significant differences in the $\delta^{18}O_{coral}$-$\delta^{18}O_{water}$ predicted at $\delta^{13}C_{coral}$-$\delta^{13}C_{DIC}$ intercept (Figure 2a). Third, there is no a priori reason why $\delta^{13}C_{coral}$-$\delta^{13}C_{DIC} = 0‰$ should be used as the point of reference for interpreting oxygen isotope fractionation as apparent equilibrium. Indeed, the carbon isotope fractionation between carbonate mineral and bicarbonate has been suggested to be $1.0 \pm 0.2‰$ [*Romanek et al.*, 1992], while a recently developed ion-by-ion model of calcite-water carbon isotope fractionation suggests that the $\delta^{13}C_{coral}$-$\delta^{13}C_{DIC}$ of abiogenic experiments will vary as a function of temperature, pH, and growth rate [*Watkins and Hunt*, 2015]. Finally, estimates of the errors in reconstructed temperature should consider analytical errors and the uncertainties in the regression slope and intercept, which will increase with extrapolation (Figure 2).

This study attempts to build upon previous work by incorporating the concepts above, with the goal of establishing a set of best practices that account for vital effects on bamboo coral δ^{18}O and δ^{13}C. It reanalyzes

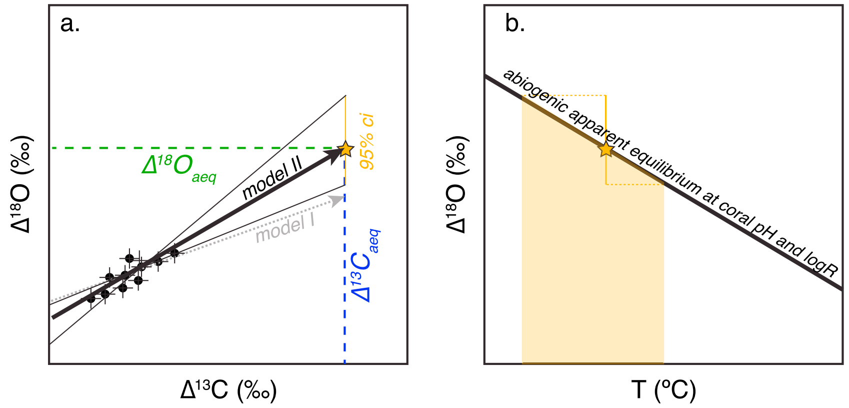

Figure 2. Schematic illustration of *Smith et al.*'s [2000] method applied to hypothetical data that include the modifications proposed in this study. (a) Model II linear regressions are extrapolated to the appropriate apparent equilibrium carbon isotope fractionation ($\Delta^{13}C_{aeq}$). Oxygen isotope fractionation at this point is assumed to be apparent equilibrium oxygen isotope fractionation ($\Delta^{18}O_{aeq}$; orange star). Uncertainty in this value is estimated from the 95% confidence interval of the regression. Using model I regressions (grey dotted line) would underestimate $\Delta^{18}O_{aeq}$. (b) If vital effects have been accounted for, coral-based $\Delta^{18}O_{aeq}$ should overlap with that of abiogenic experiments, allowing temperature to be estimated from the abiogenic temperature dependence predicted by *Watkins and Hunt* [2015] at the coral's growth rate and pH (Figure 1).

published data, using model II regressions and the most appropriate abiogenic analogs, to evaluate the degree to which the method of *Smith et al.* [2000] can correct for bamboo coral vital effects. Included in this reevaluation is a more thorough assessment of uncertainty, the error on reconstructed temperature if $\delta^{18}O_{water}$ is assumed constant, and what measures might reduce that error.

2. Materials and Methods

2.1. Data Sources

This study leverages previously published $\delta^{18}O$ and $\delta^{13}C$ data from *Isididae* corals. Data comes from two studies explicitly designed to apply the method of *Smith et al.* [2000] [*Hill et al.*, 2011; *Kimball et al.*, 2014], and one that focuses on pH-dependent boron isotope fractionation but includes sufficient $\delta^{18}O$ and $\delta^{13}C$ analyses [*Farmer et al.*, 2015a]. These specimens include Atlantic and Pacific corals from depths of 300 to 2136 m that grew at temperatures of 2.0° to 13.2°C. In most cases, corals were recently collected live, but this is not certain for select dredge specimens. The majority of $\delta^{18}O$ and $\delta^{13}C$ data were collected along radially milled transects from the coral rim to its center, although in some cases paired data derive from a coral branch or a nonbasal internode.

2.2. Notation, Regression and Comparison With Abiogenic Experiments

In this study we express carbon isotope fractionation relative to DIC using $\Delta^{13}C$ as shorthand for $1000\ln\alpha C_{calcite\text{-}DIC}$ and $\Delta^{18}O$ as shorthand for $1000\ln\alpha O_{calcite\text{-}water}$. This approach is similar to, but formally more appropriate than, values of $\delta^{18}O_{coral}$-$\delta^{18}O_{water}$ and $\delta^{13}C_{coral}$-$\delta^{13}C_{DIC}$ used previously [e.g., *Hill et al.*, 2011; *Kimball et al.*, 2014] and avoids their mixing of PDB and SMOW scales. Trends were extrapolated using standard major axis model II regression, which differs slightly from the model I regressions used previously [e.g., *Hill et al.*, 2011; *Kimball et al.*, 2014] but is technically more appropriate given that both $\Delta^{13}C$ and $\Delta^{18}O$ are dependent variables. A significant advantage of model II regression in this context is that a single slope describes the $\Delta^{13}C$ and $\Delta^{18}O$ relationship regardless of the axis on which each is plotted [*Smith*, 2009]. Only data sets with at least five data points and a significant, positive model II trend (i.e., $r > 0$; $p < 0.05$) were considered.

Evaluating $\Delta^{18}O$ at a given $\Delta^{13}C$ is intended to correct for biologically mediated vital effects and yield a $\Delta^{18}O$ value equivalent to that of abiogenic experiments precipitated under the same conditions. In other words, to make bamboo corals "look" like laboratory precipitation experiments that are unaffected by biological processes. True equilibrium oxygen isotope fractionation [e.g., *Coplen*, 2007] cannot be achieved at the growth rates of either laboratory experiments or biogenic carbonates ($\log R \approx -8.0$ to -5.0 mol/m^2/s) [*Watkins et al.*, 2013, 2014], making abiogenic experiments precipitated at the same temperature, precipitation rate, and pH [*Dietzel et al.*, 2009; *Gabitov et al.*, 2012; *Kim and O'Neil*, 1997; *Watkins et al.*, 2014] as bamboo corals the best analogs for the fractionation expected in the absence of biological effects. The phrase apparent equilibrium is used to describe this condition and is notated as $\Delta^{13}C_{aeq}$ and $\Delta^{18}O_{aeq}$. Because no existing experiment perfectly captures bamboo coral calcification conditions, trends were extrapolated to the $\Delta^{13}C_{aeq}$ value predicted by the ion-by-ion model of calcite growth developed by *Watkins and Hunt* [2015] for a specimen's modern growth temperature, pH, and growth rate (Figure 1).

Briefly, this model represents calcite growth or dissolution in terms of the attachment and detachment of ions (e.g., Ca^{2+}, HCO_3^-, and CO_3^{2-}) to the mineral surface, with growth occurring when ion attachment exceeds detachment [*DePaolo*, 2011]. Constrained by data from abiogenic precipitation experiments, the fractionation of carbon and oxygen isotopes is modeled in terms of the proportions of HCO_3^- and CO_3^{2-}, their isotopic compositions and the magnitude of fractionations associated with ion transport onto or away from the mineral surface [*Watkins et al*., 2013, 2014; *Watkins and Hunt*, 2015]. Consistent with theory, the model imposes a single equilibrium $\Delta^{13}C$ and $\Delta^{18}O$ value for a given temperature, which occurs when the rate of ion attachment approaches the rate of detachment. At faster growth rates (expressed as log *R*), where attachment exceeds detachment, kinetic effects lead to smaller fractionations of carbon and oxygen isotopes, but the degree to which fractionation decreases varies with the pH-dependent distribution of HCO_3^- and CO_3^{2-}. The model successfully explains nontemperature-dependent discrepancies among natural and laboratory calcites [e.g., *Coplen*, 2007; *Dietzel et al*., 2009; *Kim and O'Neil*, 1997; *Spero et al*., 1997] in terms of precipitation rate and pH, suggesting it is well suited to estimating bamboo coral $\Delta^{13}C_{aeq}$ and $\Delta^{18}O_{aeq}$ provided these variables can be constrained.

Such bamboo coral growth rate and pH estimates exist via radiocarbon and ^{210}Pb data [*Andrews et al*., 2009; *Farmer et al*., 2015b; *Hill et al*., 2011; *Roark et al*., 2005; *Sherwood and Edinger*, 2009], and $\delta^{11}B$ [*Farmer et al*., 2015a], respectively. Although these growth and pH estimates come with uncertainties that will propagate to bamboo coral-based paleoclimate reconstructions, the influence of these uncertainties can be quantified. This is a distinct advantage over the common approach of ignoring nontemperature effects when comparing biogenic data to abiogenic experiments, which likely yields large but unquantifiable errors.

Because much of the $\delta^{18}O$ and $\delta^{13}C$ data used in this study are not accompanied by the requisite pH and growth rate data, the median growth rate (log $R = -7.3$ mol/m^2/s) and pH (8.0) of bamboo corals in the literature (Figure 1) were used. The $\Delta^{13}C_{aeq}$ temperature dependence predicted by the ion-by-ion model for these values is

$$\Delta^{13}C_{aeq} = 1.68 \times 1000/T(°K)^2 - 4.05 \times 1000/T(°K) - 4.97 \quad (1)$$

At the median growth rate and pH of bamboo corals the complementary apparent equilibrium oxygen isotope fractionation ($\Delta^{18}O_{aeq}$) predicted by the ion-by-ion model is

$$\Delta^{18}O_{aeq} = 17.86 \times 1000/T(°K) - 30.98 \quad (2)$$

We note that the temperature sensitivity of equation (2) is very similar to that of abiogenic experiments [*Kim and O'Neil*, 1997; *Watkins et al*., 2013, 2014], but with a more positive intercept that trends toward the value expected in very slowly growing calcite crystals (<0.02 nm/s) [*Gabitov et al*., 2012]. It should also be noted that equations (1) and (2) are constructed entirely from fits to abiogenic laboratory calcite data precipitated under known conditions and are independent of bamboo coral $\Delta^{13}C$ and $\Delta^{18}O$.

Coral-based temperatures were calculated by first extrapolating linear $\Delta^{13}C$-$\Delta^{18}O$ trends to $\Delta^{13}C_{aeq}$, calculated from equation (1) using observed modern temperatures. The complementary $\Delta^{18}O$ at that point is then interpreted as $\Delta^{18}O_{aeq}$ and can be used to solve equation (2) for temperature. Although there is an inherent circularity to this approach due to the mutual temperature dependence of equations (1) and (2), the fact that the temperature sensitivity of $\Delta^{18}O_{aeq}$ approaches 3 times that of $\Delta^{13}C_{aeq}$ suggests that it may be reasonable to assume a constant $\Delta^{13}C_{aeq}$, calculated from modern temperatures, when interpreting oxygen isotope variability in paleooceanaographic context. A key advantage to this approach is that it estimates temperature from a completely independent abiogenic relationship without relying on empirical calibrations. As such, it is assumed that biological vital effects have been accounted for when this method yields coral-based temperature estimates that are within error of observed growth temperatures.

2.3. Uncertainty Estimates

The skill with which the method described above captures observed temperatures depends, in part, on the uncertainty of $\Delta^{18}O_{aeq}$ at $\Delta^{13}C_{aeq}$, which can be estimated from the 95% confidence intervals of each coral's model II regression slope and intercept. In general, uncertainty in $\Delta^{18}O_{aeq}$ will decrease with stronger linear trends and more positive Δ^{13}C values that require less extrapolation to reach $\Delta^{13}C_{aeq}$. Weaker trends that must be extrapolated over a wider range result in larger errors in $\Delta^{18}O_{aeq}$. To evaluate how uncertainty in $\Delta^{18}O_{aeq}$ affects reconstructed temperatures, we used a Monte Carlo approach to sample the 95% confidence interval of each coral's $\Delta^{18}O_{aeq}$ 10,000 times, assuming a normal distribution, to generate 10,000 coral-based temperatures. The same approach was used to sample the uncertainty of reported growth temperatures, from which the root-mean-square error (RMSE) of predicted versus observed temperature was calculated.

The assumption that each coral's calcite skeleton was precipitated at pH = 8.0 and $\log R = -7.3$ mol/m^2/s also introduces uncertainty. Quantifying this effect using existing studies is difficult due to the general absence of comprehensive pH, growth rate, δ^{13}C, and δ^{18}O data sets, but it can be explored with pseudocoral experiments. We performed a series of experiments in which an idealized Δ^{13}C versus Δ^{18}O linear trend was first generated using ion-by-ion model values for two hypothetical corals grown at pH = 8.0, $\log R = -7.3$ mol/m^2/s, and a temperature of either 4°C or 12°C. Because the magnitude of $\Delta^{18}O_{aeq}$ uncertainty introduced by a given error in $\Delta^{13}C_{aeq}$ depends on the steepness of the Δ^{13}C-Δ^{18}O trend, we considered slopes of 0.25, 0.40, and 0.80‰/‰. Furthermore, pseudocoral data sets of 10, 40, and 80 samples were considered. These ranges in slope value and sample number both generally span those of actual coral data (Table S1 in the supporting information).

Realistic noise was introduced by adding a random value to Δ^{18}O that was drawn from a normal distribution with a mean of zero and a standard deviation of either 0.0, 0.2, or 0.5‰. The latter two values approximate the observed range in Δ^{18}O regression residuals, while the obviously unrealistic zero value allows pH and log *R* uncertainty to be explored in the absence of regression errors. In each case, the influence of pH and log *R* were evaluated by randomly selecting values of ±0.2 unit (i.e., 7.8 to 8.2) and ±0.3 mol/m^2/s (i.e., -7.0 to -7.6). The pH range is realistic, given suggestions that δ^{11}B may resolve anomalies as small as 0.1 unit [*Farmer et al.*, 2015a]. The log *R* range is approximately equivalent to a precision of ±30 μm/yr, which is typical of recent bamboo coral growth rate estimates [e.g., *Farmer et al.*, 2015b]. It should be noted that in both cases the range of values tested, which reflect how well pH or growth rate may be estimated in a single coral, are distinct from the distributions in Figure 1, which indicate the variability among many corals.

For each set of randomly selected values, the Δ^{13}C-Δ^{18}O trend was extrapolated to the appropriate $\Delta^{13}C_{aeq}$, and a complementary $\Delta^{18}O_{aeq}$ value was drawn from a normal distribution defined by the 95% confidence intervals of the regression, as described above. Temperature was then calculated from the appropriate $\Delta^{18}O_{aeq}$-temperature relationship at the selected pH and log *R*. Finally, the pseudocoral-based temperature was compared with the "observed" temperature, which was randomly drawn from a normal distribution with a mean of either 4°C or 12°C and a standard deviation of 0.2°C typical of observational error. This exercise was repeated 10,000 times from which the RMSE was calculated in the same way as the actual coral data.

3. Results

From an initial compilation of 61 records, 32 were retained that had five or more data points and a significant positive trend (i.e., $r > 0$; $p < 0.05$; Table S1 in the supporting information). Most (93%) of the rejected data sets consisted of seven or fewer data points, but records from specimens PV 694-13 [*Kimball et al.*, 2014] and T668-A13 [*Farmer et al.*, 2015a] were excluded despite 29 and 21 data points, respectively. *Kimball et al.* [2014] noted the absence of a significant relationship in PV 694-13 but did not discuss its cause. Although sample T668-A13 is nearly significant ($p = 0.051$), the absence of a stronger regression may be associated with sampling transects collected with both a rotary drill and micromill.

Retained records of 5 to 73 data points exhibited correlation coefficients of 0.32 to 0.98 and *p* values of 0.046 to 10^{-30} (Table S1 in the supporting information). The slopes of model II regressions varied from 0.23 to 1.38‰/‰ and showed no obvious relationship with growth temperature. Slopes were steeper than originally published model I slopes, which produced more positive intercepts that ranged from 30.98 to 33.41‰. The 95% confidence intervals of slopes and intercepts varied from minima of 0.06‰/‰ and 0.09‰ for robust regressions to 1.67‰/‰ and 2.8‰ for weaker relationships.

Values of $\Delta^{13}C_{aeq}$ varied with coral growth temperature (equation (1)) from a maximum of 2.50‰ at the coldest sites (2°C) to a minimum of 1.37‰ at the warmest (13.2°C). Extrapolating linear trends to these $\Delta^{13}C_{aeq}$ values yielded $\Delta^{18}O_{aeq}$ estimates ranging from 31.37 ± 0.27‰ to 35.41 ± 2.63‰. When plotted against each coral's known growth temperature, most Pacific coral $\Delta^{18}O_{aeq}$ values were within error of the temperature

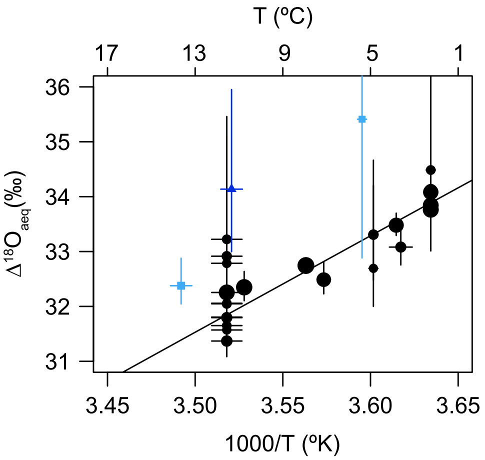

Figure 3. The temperature dependence of Pacific (black circle), recent Atlantic (light blue square), and preindustrial Atlantic (dark blue triangle) bamboo coral $\Delta^{18}O_{aeq}$ compared with the abiogenic trend at pH = 8.0 and log*R* = −7.3 mol/m^2/s (black line) [*Watkins and Hunt*, 2015]. Symbol size is scaled to regression *p* value. $\Delta^{18}O_{aeq}$ error bars reflect the 95% confidence interval of linear regressions extrapolated to $\Delta^{13}C_{aeq}$. Temperature error bars are the originally reported uncertainty in observed temperature.

dependence of abiogenic oxygen isotope fractionation (equation (2); Figure 3). Corals that deviated most severely from equation (2) typically underestimated temperature. This was true for all three Atlantic specimens, which underestimated observed temperature by 4 to 9°C.

Uncertainty in coral-based temperatures was proportional to the significance of regressions such that lower *p* values corresponded to smaller errors (Figure 4). Twenty-two percent of records had a RMSE of 2°C or less, while 47% had a value below 3°C. Temperature reconstructed from specimen BB [*Hill et al.*, 2011], which had the lowest *p* value (7.3×10^{-30}) in this study, was found to have a RMSE of only 0.65°C.

Uncertainty estimates from pseudocoral experiments show a similar relationship between *p* values and RMSE (Figure 5). All else being equal, RMSE decreased with a greater number of samples and a steeper $\Delta^{13}C$-$\Delta^{18}O$ slope, and only a subtle difference between temperatures was observed (Table S2 in the supporting information). For instances of perfect $\Delta^{13}C$-$\Delta^{18}O$ regressions, RMSE for a 4°C growth temperature varied from 0.24 to 0.42°C depending on the trend slope, with a similar range of 0.25 to 0.64°C for a 12°C growth temperature. This suggests that uncertainties in pH and growth rate introduce errors of about 0.5°C. Robust linear relationships approach this value, while weaker trends produce appreciably larger RMSEs due to larger 95% confidence intervals on $\Delta^{18}O_{aeq}$ when they are extrapolated to $\Delta^{13}C_{aeq}$. The RMSEs of pseudocoral experiments generally bound those of actual coral data (Figure 4), and it is noteworthy that the robust relationship in specimen BB produces a RMSE that approaches the ~0.5°C value predicted for pH and growth rate uncertainty alone.

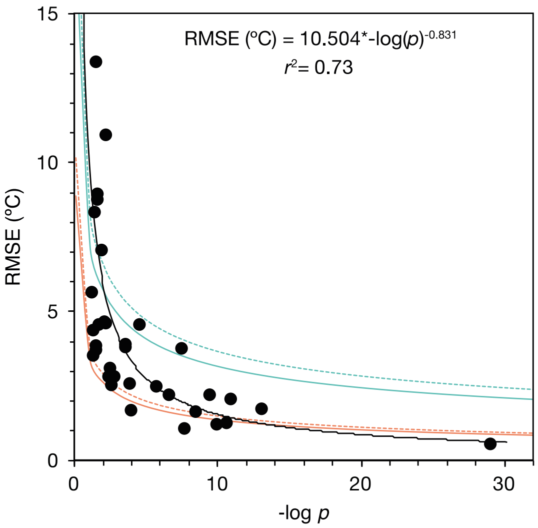

Figure 4. Monte Carlo-based RMSE of coral-based reconstructed temperature (black circle) plotted against the negative log of regression *p* value. Equivalent results for pseudocoral experiments at 4°C (dashed line) and 12°C (solid line) are shown for cases where the standard deviation of $\Delta^{18}O$ regression residuals was 0.2‰ (red) or 0.5‰ (blue).

4. Discussion

4.1. Choosing Appropriate Apparent Equilibrium Values

The success with which the *Smith et al.* [2000] method corrects for vital effects relies on extrapolating $\Delta^{13}C$-$\Delta^{18}O$ trends to the appropriate $\Delta^{13}C_{aeq}$ value and comparing the $\Delta^{18}O$ at that value to the appropriate relationship for the temperature dependence of oxygen isotope fractionation at apparent equilibrium. *Smith et al.* [2000] used a $\Delta^{13}C_{aeq}$ of 0‰ for aragonitic deep sea corals that were ~2.7‰ more negative than the value suggested by *Romanek et al.* [1992] largely because it resulted in good agreement between their predicted $\Delta^{18}O_{aeq}$ and

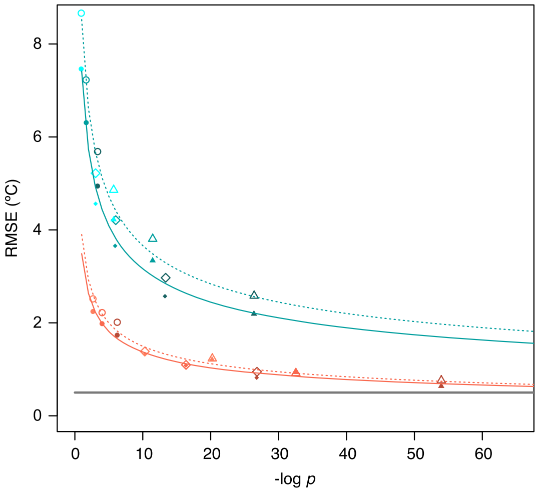

Figure 5. As in Figure 4 for pseudocoral experiments in which the standard deviation of $\Delta^{18}O$ regression residuals was 0.2‰ (red) or 0.5‰ (blue). Experiments considered synthetic data sets of 10 (circles), 40 (diamonds), or 80 (triangles) samples, with $\Delta^{13}C$-$\Delta^{18}O$ slopes of 0.25 (light color), 0.40 (medium color), or 0.80 (dark color) ‰/‰ and growth temperatures of 4 (open) and 12°C (closed). The horizontal black line marks the ~0.5°C limit set by uncertainty in pH and growth rate estimates for experiments with perfect linear trends. See Table S2 in the supporting information.

the temperature-dependent oxygen isotope fractionation observed in aragonitic foraminifera and mollusks [*Grossman and Ku*, 1986].

This choice was rationalized by suggesting that it reflected a small incorporation of ^{13}C depleted carbon from respired CO_2, but the recent work of *Watkins and Hunt* [2015] suggests that it could also partially reflect the correction factor necessary to account for different calcifying pH values and growth rates between these organisms.

Hill et al. [2011] and *Kimball et al.* [2014] adopted the same $\Delta^{13}C_{aeq}$ of 0‰ for calcitic bamboo corals despite evidence for a ~1.7‰ difference in apparent equilibrium carbon isotope fractionation between calcite and aragonite [*Romanek et al.*, 1992]. Equation (1) suggests that a $\Delta^{13}C_{aeq}$ of 0‰ underestimates the true value for typical bamboo coral growth conditions by up to 2.5‰, thereby underestimating $\Delta^{18}O_{aeq}$ and contributing to the offset between the empirical coral-based $\Delta^{18}O$-temperature relationship and that of *Kim and O'Neil's* [1997] abiogenic experiments. This problem would have been exacerbated by the shallower slopes of the model I regressions employed by *Hill et al.* [2011] and *Kimball et al.* [2014]. However, it should be noted that equation (2) also predicts $\Delta^{18}O_{aeq}$ values that are higher than those of *Kim and O'Neil* [1997] at a given temperature, likely because typical bamboo coral growth rates are slower than the precipitation rate of Kim and O'Neil's experimental calcites. Thus, the previously reported offset between coral-based and abiogenic $\Delta^{18}O$-temperature relationships was likely caused by selecting both $\Delta^{13}C_{aeq}$ and $\Delta^{18}O_{aeq}$ values that did not reflect the fractionations expected at the temperature, pH, and growth rate of bamboo coral calcification, and further complicated by the use of model I regressions.

This study's use of $\Delta^{13}C_{aeq}$ and $\Delta^{18}O_{aeq}$ values that are appropriate abiogenic analogs for bamboo coral calcification conditions (equations (1) and (2)) alleviates the disagreement between coral-based and abiogenic $\Delta^{18}O$-temperature relationships for most specimens, particularly those in the Pacific. This suggests that the biological processes responsible for large carbon and oxygen isotope disequilibria in bamboo corals have been accounted for and that coral-based fractionation factors have been made equivalent to abiogenic experiments precipitated at the same temperature, pH, and growth rate. As such it is appropriate to estimate coral growth temperature from the completely independent abiogenic relationship (equation (2)) in Pacific specimens, eliminating the use of an empirical calibration. Our pseudocoral experiments suggest that errors in growth rate and pH estimates contribute uncertainty of about ±0.5°C to coral-based temperatures but that the strength of $\Delta^{13}C_{aeq}$-$\Delta^{18}O_{aeq}$ regressions is often the major determining factor in the method's skill. Atlantic corals typically exhibit higher than expected $\Delta^{18}O_{aeq}$ estimates that are difficult to explain in terms of pH or growth rate, and possible explanations for this are discussed below.

4.2. Respired CO_2

Although the $\Delta^{13}C_{aeq}$ and $\Delta^{18}O_{aeq}$ values predicted by the model of *Watkins and Hunt* [2015] appear to describe most bamboo corals relatively well, they would not account for ^{13}C depleted carbon from respired CO_2 if it were incorporated into their skeletons as suggested by *Smith et al.* [2000]. The incorporation of respired CO_2 would decrease $\Delta^{13}C$ values, and because the $\Delta^{13}C_{aeq}$ predicted by equation (1) would be the same, would result in a higher $\Delta^{18}O_{aeq}$. This is consistent with the higher $\Delta^{18}O_{aeq}$ of Atlantic specimens.

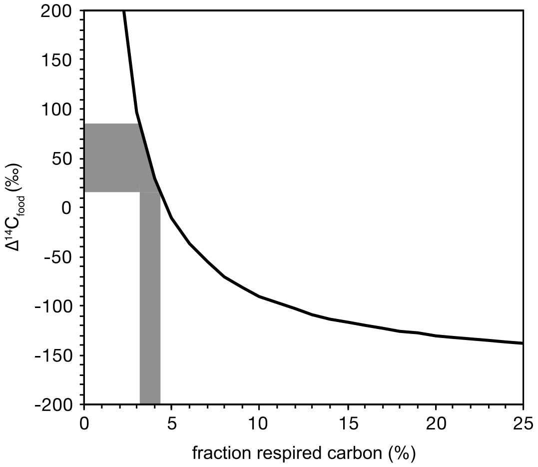

Figure 6. Evaluation of the fraction of skeletal carbon that could derive from metabolic CO_2 (f) for a Gulf of Alaska bamboo coral [*Roark et al.*, 2005] compared with reasonable estimates of the $\Delta^{14}C$ of its food source. Using equation (4) (black line) and assuming $\Delta^{14}C_{food}$ values between surface DIC and POC suggests an f of 3−5%.

However, the radiocarbon content of bamboo coral skeletons indicates that calcite carbon derives almost exclusively from ambient DIC [*Farmer et al.*, 2015b; *Hill et al.*, 2011; *Roark et al.*, 2005], which is inconsistent with an appreciable contribution from respired CO_2. Thus, to evaluate if respired CO_2 could contribute to the higher than predicted $\Delta^{18}O_{aeq}$ in Atlantic corals, it is first necessary to demonstrate that respired CO_2 could be incorporated into any bamboo coral skeleton.

To this end, a mass balance approach [*Adkins et al.*, 2003] was employed using data from a Warwick Seamount site with a relatively complete data set. This approach estimates the maximum contribution of respired CO_2 to coral skeleton based on the radiocarbon content of skeleton, food source, and ambient DIC:

$$\Delta^{14}C_{coral} = f \times \Delta^{14}C_{food} + (1 - f) \times \Delta^{14}C_{DIC} \tag{3}$$

where f is the fraction of respired carbon. Equation (3) can be rearranged to solve for $\Delta^{14}C_{food}$:

$$\Delta^{14}C_{food} = \left(\Delta^{14}C_{coral} - \Delta^{14}C_{DIC}\right)/f + \Delta^{14}C_{DIC} \tag{4}$$

Roark et al. [2005] report a $\Delta^{14}C_{coral}$ of −162‰ for bamboo coral ALV 3808-3 and a $\Delta^{14}C_{DIC}$ of −170‰, suggesting a maximum $\Delta^{14}C_{coral}$-$\Delta^{14}C_{DIC}$ of ~8‰. If the radiocarbon content of food is estimated to fall between that of surface $\Delta^{14}C_{DIC}$ (18‰) [*Roark et al.*, 2005] and surface particulate organic carbon (POC), which has a $\Delta^{14}C$ 70‰ higher than surface $\Delta^{14}C_{DIC}$ (i.e., 88‰) [*Druffel et al.*, 1986], solving equation (4) for f suggests that at most 3–5% of skeletal carbon derives from respired CO_2 at this site (Figure 6).

A similar mass balance for $\delta^{13}C$ can then be written:

$$\delta^{13}C_{coral} = f \times \delta^{13}C_{c\text{-}res} + (1 - f) \times \delta^{13}C_{c\text{-}DIC} \tag{5}$$

where $\delta^{13}C_{c\text{-}res}$ is the isotopic composition of skeletal calcite derived from respired CO_2 and $\delta^{13}C_{c\text{-}DIC}$ is the equivalent value for calcite derived from ambient DIC. A $\delta^{13}C_{DIC}$ of −0.71‰ [*Guilderson et al.*, 2006], and the $\Delta^{13}C_{aeq}$ of 2.32‰ (equation (1)), calculate $\delta^{13}C_{c\text{-}DIC}$ to be 1.61‰. If the $\delta^{13}C$ of respired CO_2 is assumed to equal the POC value of −25‰ [*Druffel et al.*, 1986], the temperature-dependent calcite-CO_2 carbon isotope fractionation factor of *Romanek et al.* [1992] predicts $\delta^{13}C_{c\text{-}res}$ to be −13.75‰ at the 3.7°C growth temperature of ALV 3803-3. Solving equation (5) with an f of 4% then predicts $\delta^{13}C_{coral}$ to be 1.00‰, which can be used to calculate $\Delta^{13}C_{coral}$ to be 1.70‰. Extrapolating ALV 3808-3 $\Delta^{13}C$-$\Delta^{18}O$ trends to this value yields a $\Delta^{18}O_{aeq}$ of 33.72 ± 0.71‰, from which equation (2) predicts a temperature of 2.9 ± 3.0°C that compares well with the observed value of 3.7°C. In contrast, the assumption that $f = 0$%, predicts a $\Delta^{18}O_{aeq}$ of 33.93 ± 0.81‰ and a temperature of 2.0 ± 3.4°C. Although temperature uncertainties make any conclusion equivocal, the calculations above do suggest that a small incorporation of carbon from respired CO_2 is plausible for bamboo corals and could help explain Atlantic data as well as some of the scatter of coral-based $\Delta^{18}O_{aeq}$ about the abiogenic trend in other specimens (Figure 3). Unfortunately, the $\Delta^{14}C$ data necessary to constrain f using equation (4) are not available at most sites, including those in the Atlantic.

In spite of the absence of $\Delta^{14}C$ data, the potential role of respired CO_2 can be explored using equation (5) across a reasonably wide range of f values from 0 to 15%. This was done for all 32 coral records, and $\Delta^{18}O_{aeq}$ calculated at each f value was compared to the abiogenic relationship. The f for which agreement

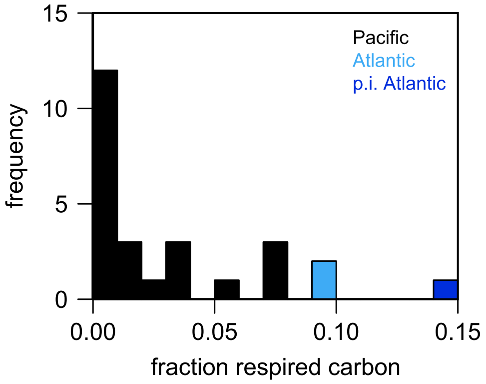

Figure 7. Histogram of the *f* value that produces the best agreement between each coral-based $\Delta^{18}O_{aeq}$ and the abiogenic value at each coral's growth temperature for Pacific (black), recent Atlantic (light blue), and pre-industrial Atlantic (dark blue) specimens.

was best was then recorded. The best agreement occurred at $f = 0\%$ for the majority of Pacific samples (Figure 7), supporting previous evidence that most bamboo corals precipitate their skeleton nearly exclusively from ambient DIC [e.g., *Roark et al.*, 2005]. Samples for which higher *f* values produce better agreement with observations do not show a consistent relationship with temperature, depth, or the strength of linear trends, but hypothetically may be explained by species-specific increases in respired carbon incorporation or $\delta^{13}C_{c\text{-res}}$ that are not captured by relatively uncertain bamboo coral classification [*Watling et al.*, 2011]. In particular, Atlantic specimens suggest especially high *f* values (9–15%) that could reflect regional, species-specific behavior. However, at least one of these specimens (BE1) [*Hill et al.*, 2011] was not collected alive and may also be affected by diagenesis. A radiocarbon data set equivalent to that of ALV 3808-3 from Atlantic sites and rigorous diagenetic screening would be necessary to distinguish between these possibilities. Although respired CO_2 remains a viable mechanism to explain the offset in Atlantic coral and abiogenic $\Delta^{18}O_{aeq}$, it should be noted that in most cases it is reasonable to assume no respired carbon is incorporated into Pacific coral skeletons when *f* cannot be calculated independently.

4.3. The Skill of Temperature Reconstructions

Even when appropriate $\Delta^{13}C_{aeq}$ and $\Delta^{18}O_{aeq}$ values and model II regressions are used, the method of *Smith et al.* [2000] will include errors from estimating pH and growth rate, extrapolating trends, and from uncertainties in observed temperature that will reduce the skill of paleotemperature reconstructions. When these effects are considered, the uncertainty in coral-based temperature is usually higher than those based only on the regression error of empirical calibrations [*Hill et al.*, 2011; *Kimball et al.*, 2014]. However, we believe our method yields more honest uncertainty estimates that acknowledge that the isotopic signatures of bamboo corals are controlled by multiple variables and attempts to quantify their effects on paleotemperature estimates. Despite this more comprehensive assessment of uncertainty, it is noteworthy that the most significant relationship (BB) [*Hill et al.*, 2011] achieves a RMSE of ~0.65°C that is similar to previously suggested uncertainty estimates and close to the pseudocoral-based limit set by the current ability to estimate pH and growth rate. The strong relationship between RMSE and *p* value (Figure 4) indicates that dozens of samples are likely required, but not necessarily sufficient, to achieve this skill. Although strict rules cannot be made for the minimum number of samples, it is instructive to note that the RMSE for regressions based on greater than 50 samples averaged 1.4°C, while that of regressions based on six or fewer samples was 5.0°C.

The proportionality between RMSE and *p* value (Figures 4 and 5) is also significant in that it may provide a means of estimating temperature uncertainty for fossil bamboo corals with unknown growth temperatures. If the relationship in Figure 4 is maintained as it is populated by more modern specimens, it could be used to derive empirical RMSE estimates using only the $\Delta^{13}C$-$\Delta^{18}O$ regression *p* values in fossil specimens. Such measures of skill are critical for accurate paleoclimatic interpretations and help ensure that small anomalies in proxy records are not overinterpreted.

5. Conclusions and Outlook

This study demonstrates that linear correlations in $\Delta^{13}C$-$\Delta^{18}O$ can be used to extract meaningful paleotemperature estimates from bamboo corals using abiogenic relationships rather than empirical calibrations when fractionation factors and regression methods are chosen carefully. Typical temperature errors of $\pm 2-3$°C are capable of resolving the largest temperature variations, such as the >5°C subsurface anomalies that accompany El Niño events. Data sets with many analyses and strong linear relationships may resolve more subtle temperature anomalies such as those that characterize much of the intermediate ocean.

Fractionation factors are controlled by multiple variables however, and the skill with which temperature can be reconstructed will depend on how well these variables can be constrained or assumed constant. For example, capturing even large temperature anomalies will be contingent on $\delta^{18}O_{water}$ and $\delta^{13}C_{DIC}$ remaining relatively constant, and appreciable variations in either value will add uncertainty to paleotemperature estimates. Similarly, the mutual temperature dependence of equations (1) and (2) could complicate paleotemperature reconstructions, but given that the temperature sensitivity of $\Delta^{18}O_{aeq}$ is approximately 3 times that of $\Delta^{13}C_{aeq}$, it will likely be reasonable to make the simplifying assumption to calculate $\Delta^{13}C_{aeq}$ using modern climatological temperatures. Alternatively, the development of independent paleotemperature proxies may allow the method to be inverted to solve for variations in $\delta^{18}O_{water}$ and $\delta^{13}C_{DIC}$. In any case, the most robust results will likely be achieved when pH and growth rate are estimated from $\delta^{11}B$ and $\Delta^{14}C$, respectively, for each coral, rather than assuming an average value for all specimens. Any improvements in the precision with which these proxies estimate pH and growth rate will also improve the maximum skill achievable by robust linear $\Delta^{13}C$-$\Delta^{18}O$ trends. Radiocarbon measurements in surface skeleton and local DIC and POC will also help constrain the degree to which $\Delta^{13}C_{aeq}$ may be altered by respired CO_2, thereby potentially improving paleotemperature estimates and gaining insight on regional variations in bamboo coral growth strategies.

Despite the promising results from this study, future work is warranted to improve confidence in bamboo coral-based paleoclimate records. In particular, a suite of diverse corals should be densely sampled with the goal of generating the most robust linear relationships. This work should be complemented by constraining as many of the variables above as possible for individual specimens. Such work will help establish a more robust understanding of the strengths and limitations of reconstructing past climates using the unique bamboo coral archive.

Acknowledgments
C.S. is grateful for financial support from the University of Washington Oceanography Department and laboratory assistance from Andy Schauer. This study would not have been possible without the hard work of previous researchers, and their data used here are listed in the references, tables, and supporting information. We also thank two anonymous reviewers, whose comments improved this manuscript.

References

Adkins, J. F., E. A. Boyle, W. B. Curry, and A. Lutringer (2003), Stable isotopes in deep-sea corals and a new mechanism for “vital effects”, *Geochim. Cosmochim. Acta*, *67*, 1129–1143, doi:10.1016/S0016-7037(02)01203-6.

Andrews, A. H., R. P. Stone, C. C. Lundstrom, and A. P. DeVogelaere (2009), Growth rate and age determination of bamboo corals from the northeastern Pacific Ocean using refined 210Pb dating, *Mar. Ecol. Prog. Ser.*, *397*, 173–185, doi:10.3354/meps08193.

Bond, Z. A., A. L. Cohen, S. R. Smith, and W. J. Jenkins (2005), Growth and composition of high-Mg calcite in the skeleton of a Bermudian gorgonian (Plexaurella dichotoma): Potential for paleothermometry, *Geochem. Geophys. Geosyst.*, *6*, Q08010, doi:10.1029/2005GC000911.

Chen, X., and K.-K. Tung (2014), Varying planetary heat sink led to global-warming slowdown and acceleration, *Science*, *345*, 897–903, doi:10.1126/science.1254937.

Coplen, T. B. (2007), Calibration of the calcite–water oxygen-isotope geothermometer at Devils Hole, Nevada, a natural laboratory, *Geochim. Cosmochim. Acta*, *71*, 3948–3957, doi:10.1016/j.gca.2007.05.028.

DeFoe, O. K., and A. H. Compton (1925), The density of rock salt and calcite, *Phys. Rev.*, *25*, 618–620, doi:10.1103/PhysRev.25.618.

DePaolo, D. J. (2011), Surface kinetic model for isotopic and trace element fractionation during precipitation of calcite from aqueous solutions, *Geochim. Cosmochim. Acta*, *75*, 1039–1056, doi:10.1016/j.gca.2010.11.020.

Dietzel, M., J. Tang, A. Leis, and S. J. Köhler (2009), Oxygen isotopic fractionation during inorganic calcite precipitation—Effects of temperature, precipitation rate and pH, *Chem. Geol.*, *268*, 107–115, doi:10.1016/j.chemgeo.2009.07.015.

Druffel, E. R. M., S. Honjo, S. Griffin, and C. S. Wong (1986), Radiocarbon in particulate matter from the Eastern sub-Arctic Pacific Ocean: Evidence of source of terrestrial carbon to the deep sea, *Radiocarbon*, *28*(2A), 397–407.

Emiliani, C., J. H. Hudson, E. A. Shinn, and R. Y. George (1978), Oxygen and carbon isotopic growth record in a reef coral from the Florida keys and a deep-sea coral from blake plateau, *Science*, *202*, 627–629, doi:10.1126/science.202.4368.627.

Etnoyer, P., and L. E. Morgan (2005), Habitat-forming deep-sea corals in the Northeast Pacific Ocean, in *Cold-Water Corals and Ecosystems*, *Erlangen Earth Conf. Ser.*, edited by P. D. A. Freiwald and D. J. M. Roberts, pp. 331–343, Springer, Berlin.

Farmer, J. R., B. Hönisch, L. F. Robinson, and T. M. Hill (2015a), Effects of seawater-pH and biomineralization on the boron isotopic composition of deep-sea bamboo corals, *Geochim. Cosmochim. Acta*, *155*, 86–106, doi:10.1016/j.gca.2015.01.018.

Farmer, J. R., L. F. Robinson, and B. Hönisch (2015b), Growth rate determinations from radiocarbon in bamboo corals (genus Keratoisis), *Deep Sea Res., Part I*, *105*, 26–40, doi:10.1016/j.dsr.2015.08.004.

Gabitov, R. I., E. B. Watson, and A. Sadekov (2012), Oxygen isotope fractionation between calcite and fluid as a function of growth rate and temperature: An in situ study, *Chem. Geol.*, *306–307*, 92–102, doi:10.1016/j.chemgeo.2012.02.021.

Grossman, E. L., and T.-L. Ku (1986), Oxygen and carbon isotope fractionation in biogenic aragonite: Temperature effects, *Chem. Geol.*, *59*, 59–74, doi:10.1016/0168-9622(86)90057-6.

Guilderson, T. P., E. B. Roark, P. D. Quay, S. F. Page, and C. Moy (2006), Seawater radiocarbon evolution in the Gulf of Alaska: 2002 observations, *Radiocarbon*, *48*, 1–15, doi:10.2458/azu_js_rc.48.2844.

Hill, T. M., H. J. Spero, T. Guilderson, M. LaVigne, D. Clague, S. Macalello, and N. Jang (2011), Temperature and vital effect controls on bamboo coral (Isididae) isotope geochemistry: A test of the “lines method”, *Geochem. Geophys. Geosyst.*, *12*, Q04008, doi:10.1029/2010GC003443.

Hill, T. M., M. LaVigne, H. J. Spero, T. Guilderson, B. Gaylord, and D. Clague (2012), Variations in seawater Sr/Ca recorded in deep-sea bamboo corals, *Paleoceanography*, *27*, PA3202, doi:10.1029/2011PA002260.

Hill, T. M., C. R. Myrvold, H. J. Spero, and T. P. Guilderson (2014), Evidence for benthic–pelagic food web coupling and carbon export from California margin bamboo coral archives, *Biogeosciences*, *11*, 3845–3854, doi:10.5194/bg-11-3845-2014.

Kim, S.-T., and J. R. O'Neil (1997), Equilibrium and nonequilibrium oxygen isotope effects in synthetic carbonates, *Geochim. Cosmochim. Acta*, *61*, 3461–3475, doi:10.1016/S0016-7037(97)00169-5.

Kimball, J. B., R. B. Dunbar, and T. P. Guilderson (2014), Oxygen and carbon isotope fractionation in calcitic deep-sea corals: Implications for paleotemperature reconstruction, *Chem. Geol.*, *381*, 223–233, doi:10.1016/j.chemgeo.2014.05.008.

LaVigne, M., T. M. Hill, H. J. Spero, and T. P. Guilderson (2011), Bamboo coral Ba/Ca: Calibration of a new deep ocean refractory nutrient proxy, *Earth Planet. Sci. Lett.*, *312*, 506–515, doi:10.1016/j.epsl.2011.10.013.

Levitus, S., et al. (2012), World ocean heat content and thermosteric sea level change (0–2000 m), 1955–2010, *Geophys. Res. Lett.*, *39*, L10603, doi:10.1029/2012GL051106.

McConnaughey, T. (1989), ^{13}C and ^{18}O isotopic disequilibrium in biological carbonates: I. Patterns, *Geochim. Cosmochim. Acta*, *53*, 151–162, doi:10.1016/0016-7037(89)90282-2.

Mucci, A. (1987), Influence of temperature on the composition of magnesian calcite overgrowths precipitated from seawater, *Geochim. Cosmochim. Acta*, *51*, 1977–1984, doi:10.1016/0016-7037(87)90186-4.

Oomori, T., H. Kaneshima, Y. Maezato, and Y. Kitano (1987), Distribution coefficient of Mg^{2+} ions between calcite and solution at 10–50°C, *Mar. Chem.*, *20*, 327–336, doi:10.1016/0304-4203(87)90066-1.

Roark, E. B., T. P. Guilderson, S. Flood-Page, R. B. Dunbar, B. L. Ingram, S. J. Fallon, and M. McCulloch (2005), Radiocarbon-based ages and growth rates of bamboo corals from the Gulf of Alaska, *Geophys. Res. Lett.*, *32*, L04606, doi:10.1029/2004GL021919.

Robinson, L. F., J. F. Adkins, N. Frank, A. C. Gagnon, N. G. Prouty, E. Brendan Roark, and T. van de Flierdt (2014), The geochemistry of deep-sea coral skeletons: A review of vital effects and applications for palaeoceanography, *Deep Sea Res., Part II*, *99*, 184–198, doi:10.1016/j.dsr2.2013.06.005.

Romanek, C. S., E. L. Grossman, and J. W. Morse (1992), Carbon isotopic fractionation in synthetic aragonite and calcite: Effects of temperature and precipitation rate, *Geochim. Cosmochim. Acta*, *56*, 419–430, doi:10.1016/0016-7037(92)90142-6.

Sherwood, O. A., and E. N. Edinger (2009), Ages and growth rates of some deep-sea gorgonian and antipatharian corals of Newfoundland and Labrador, *Can. J. Fish. Aquat. Sci.*, *66*, 142–152.

Sherwood, O. A., J. M. Heikoop, D. J. Sinclair, D. B. Scott, M. J. Risk, C. Shearer, and K. Azetsu-Scott (2005), Skeletal Mg/Ca in *Primnoa resedaeformis*: Relationship to temperature?, in *Cold-Water Corals and Ecosystems*, *Erlangen Earth Conf. Ser*., edited by P. D. A. Freiwald and D. J. M. Roberts, pp. 1061–1079, Springer, Berlin.

Sinclair, D. J., B. Williams, G. Allard, B. Ghaleb, S. Fallon, S. W. Ross, and M. Risk (2011), Reproducibility of trace element profiles in a specimen of the deep-water bamboo coral *Keratoisis* sp., *Geochim. Cosmochim. Acta*, *75*, 5101–5121, doi:10.1016/j.gca.2011.05.012.

Smith, J. E., H. P. Schwarcz, M. J. Risk, T. A. McConnaughey, and N. Keller (2000), Paleotemperatures from deep-sea corals: Overcoming "vital effects", *Palaios*, *15*, 25–32, doi:10.1669/0883-1351(2000)015<0025:PFDSCO>2.0.CO;2.

Smith, R. J. (2009), Use and misuse of the reduced major axis for line-fitting, *Am. J. Phys. Anthropol.*, *140*, 476–486, doi:10.1002/ajpa.21090.

Spero, H. J., J. Bijma, D. W. Lea, and B. E. Bemis (1997), Effect of seawater carbonate concentration on foraminiferal carbon and oxygen isotopes, *Nature*, *390*, 497–500, doi:10.1038/37333.

Thresher, R., S. R. Rintoul, J. A. Koslow, C. Weidman, J. Adkins, and C. Proctor (2004), Oceanic evidence of climate change in southern Australia over the last three centuries, *Geophys. Res. Lett.*, *31*, L07212, doi:10.1029/2003GL018869.

Thresher, R. E., C. M. MacRae, N. C. Wilson, and S. Fallon (2009), Feasibility of age determination of deep-water bamboo corals (Gorgonacea; Isididae) from annual cycles in skeletal composition, *Deep Sea Res., Part I*, *56*, 442–449, doi:10.1016/j.dsr.2008.10.003.

Thresher, R. E., N. C. Wilson, C. M. MacRae, and H. Neil (2010), Temperature effects on the calcite skeletal composition of deep-water gorgonians (Isididae), *Geochim. Cosmochim. Acta*, *74*, 4655–4670, doi:10.1016/j.gca.2010.05.024.

Watkins, J. M., and J. D. Hunt (2015), A process-based model for non-equilibrium clumped isotope effects in carbonates, *Earth Planet. Sci. Lett.*, *432*, 152–165, doi:10.1016/j.epsl.2015.09.042.

Watkins, J. M., L. C. Nielsen, F. J. Ryerson, and D. J. DePaolo (2013), The influence of kinetics on the oxygen isotope composition of calcium carbonate, *Earth Planet. Sci. Lett.*, *375*, 349–360, doi:10.1016/j.epsl.2013.05.054.

Watkins, J. M., J. D. Hunt, F. J. Ryerson, and D. J. DePaolo (2014), The influence of temperature, pH, and growth rate on the δ^{18}O composition of inorganically precipitated calcite, *Earth Planet. Sci. Lett.*, *404*, 332–343, doi:10.1016/j.epsl.2014.07.036.

Watling, L., S. C. France, E. Pante, and A. Simpson (2011), Biology of deep-water octocorals, *Adv. Mar. Biol.*, *60*, 41–122, doi:10.1016/B978-0-12-385529-9.00002-0.

Weinbauer, M. G., F. Brandstätter, and B. Velimirov (2000), On the potential use of magnesium and strontium concentrations as ecological indicators in the calcite skeleton of the red coral (*Corallium rubrum*), *Mar. Biol.*, *137*, 801–809, doi:10.1007/s002270000432.